Postprint of: LWT - Food Science and Technology (114): Article number 108424 (2019)

JOURNAL: LWT-FOOD SCIENCE AND TECHNOLOGY

VOLUME 114, YEAR 2019

DOI: 10.1016/j.lwt.2019.108424

A COMPARISON OF MICROFLUIDIZATION AND SONICATION TO OBTAIN NANOMETRIC ECOLOGICAL EMULSIONS. EFFECT OF DIUTAN GUM CONCENTRATION AS STABILIZER.

Jenifer Santos[1], Manuel Jiménez[1], Nuria Calero[1*], Tomas Undabeytia[2] and José Muñoz[1].

[1]Departamento de Ingeniería Química. Facultad de Química. Universidad de Sevilla c/ P. García González, 1, E41012, Sevilla, Spain.

[2]Instituto de Recursos Naturales y Agrobiología (CSIC), Apdo. 1052, 41080-Sevilla, Spain.

* Corresponding author. Tel.: +34 954 557179. *E-mail address*: nuriacalero@us.es

Abstract

The objective of this work was to develop emulsions formulated with natural ingredients such as lemongrass essential oil and Appyclean 6552 (emulsifier), aiming to reach nanometric size droplets. The emulsions were prepared using two different processing techniques: microfluidization and sonication. Sonication demonstrated to be a powerful technique to produce nanoemulsions since even an excess of energy input did not promote recoalescence, conversely to microfluidization. Despite the fact microfluidization led to recoalescence phenomenon, the results obtained in terms of droplet sizes and stability were better at lower homogenization pressures than those obtained by sonication. The best nanoemulsion concerning physical stability resulting from microfluidization process was used as a reference to incorporate diutan gum, which reduces the creaming destabilization mechanism. However, an excess above 0.3 wt% diutan gum proved counterproductive for droplet size reaching values out of nanometric scale.

Keywords: Microfluidization, sonication, lemongrass essential oil, long-term stability, diutan gum, rheology.

1. Introduction

Droplet size distribution (DSD) of emulsions is a key parameter for the stability and rheology of these dispersed systems. For example, nanoemulsions present enhanced physical stability compared to emulsions with higher droplet size. DSD is mainly governed by homogenization method used although formulation also influences. There are several high-energy methods to develop emulsions such as rotor-stators, sonicators, high-pressure pump homogenizers, colloids mills and microfluidizers. On the one hand, in the last ten years, Microfluidizers have attracted a lot of attention due to its ability to reduce droplet size [1–3]. This device is based on forcing the sample by high pressure (up to 150 MPa) through microchannels toward an impingement area. It creates an enormous shearing action, which can produce very fine emulsions. Some researchers claim that microfluidization is superior than traditional emulsifying homogenizers because the DSD obtained are narrower and smaller [4,5]. However, the use of microfluidizers is sometimes related to the over-processing phenomenon, which provokes the occurrence of re-coalescence [6]. On the other hand, the use of sonication technique in order to reduce the droplet size of emulsions presents some advantages such as the minimum recoalescence and the easiness for cleaning and servicing [7,8] . An increase of ultrasonic power or amplitude applied is directly related to the reduction of the droplet size since high amplitudes generates strong shear forces. This technique has been previously used in the production of nanoemulsions formulated with triglycerides, diazino or mucilage [9–11].

The use of essential oils as natural food preservatives has attracting attention nowadays due to their properties such as strong antioxidant, anti-inflammatory, diuretic, analgesic and antimicrobial activities among others [12,13]. Lemongrass essential oil derived from *Cymbopogon citratus* possesses several applications in food, biomedical and pharmaceutical fields [14–16]. Recent studies reveal that the antimicrobial activity of lemongrass essential oil increases with emulsion droplet size decreases [17]. This fact highlights the importance of the droplet size obtained by processing and formulation control.

Other ingredients that are contributing to development of natural products are the surfactants derived from biomass. Appyclean 6552, which belongs to the alkyl poly pentosides family, is a novel surfactant that come from a renewable raw material (wheat biomass). In addition, it is a sustainable solution to an agricultural waste such as wheat straw and possesses the ECOCERT certification. As a consequence, this emulsifier has recently incorporated in green formulations [18].

Emulsions are thermodynamically unstable systems that can suffer different destabilization mechanisms such as creaming, coalescence, Ostwald ripening and/or flocculation. The incorporation of polysaccharides as stabilizers and thickeners is very common in emulsion field in order to develop stable emulsions. Diutan gum, secreted by *Sphingomonas sp*., is an aqueous microbial polysaccharide that is considered biodegradable and biocompatible. This novel thickener has been used recently to avoid droplet size increment in alkane nanoemulsions [19]. However, to the best of our knowledge, there is a lack of information about the reduction of creaming in nanoemulsions containing essential oils by using diutan gum.

The principal aim of this study was to develop stable emulsions using materials derived from renewable resources. Furthermore, other important objective was to compare two different emulsification methods (microfluidization and sonication) on the basis of physical stability and droplet size distributions for lemongrass-in-water emulsions. In addition, the role of diutan gum in order to reduce creaming was analysed using rheological and laser diffraction measurements as well as multiple light scattering technique.

2. Materials and methods

2.1. Materials

The dispersed phase used was lemongrass essential oil, which was provided by Sigma Chemical Company. Appyclean 6552, an ecological surfactant, was supplied by Wheatoleo. All emulsions were prepared with deionized water.

2.2. Methods

Emulsions preparation

Emulsions containing 5 wt% of lemongrass essential oil and 0.5 wt% of appyclean 6552 were prepared via different emulsification methods. However, the formation of the coarse emulsion was the same: this emulsion was prepared using a Silverson L5M at 4000 rpm for 1 minute. Subsequently, different emulsions were developed as described in table 1.

Table 1. Preparation methodology for lemongrass nanoemulsions.

Samples	Technique	Homogenization pressure (psi)	Number of cycles
1	Microfluidization	2500	I
2		2500	II
3		5000	I
4		5000	II
5		10000	I
6		10000	II

7		15000	I
8		15000	II
		Amplitude (W)	**time (min)**
9		32	3
10		44	3
11		57	3
12		75	3
13	**Sonication**	85	3
14		75	1
15		75	4
16		75	5
17		75	7

Diutan gum preparation and incorporation to the nanoemulsion

A stock of 1 wt% of diutan gum solution was prepared using a IKA-Visc at 700 rpm for 3 h at room temperature. Subsequently, the dispersion was stirred at 300 rpm for 2 h in order to remove bubbles. The incorporation of diutan gum solution to the nanoemulsion selected was carried out by mixing both systems using an IKA-Visc homogenizer at 300 rpm until complete homogenization.

Laser diffraction measurements

Malvern Mastersizer 2000 was used in order to analyse the droplet size distributions for the nanoemulsions developed. The measurements were made by triplicate. In order to evaluate the results obtained, Sauter diameter and span parameter were calculated as follows:

$$D_{3,2} = \sum_{i=1}^{N} n_i d_i^3 / \sum_{i=1}^{N} n_i d_i^2 \qquad \text{Eq. (1)}$$

$$span = \frac{D_{90} - D_{10}}{D_{50}} \qquad \text{Eq. (2)}$$

Where d_i is the droplet diameter, N is the total number of droplets, n_i is the number of droplets having a diameter d_i, and D_{90}, D_{50}, D_{10} are the diameters at 90%, 50% and 10% cumulative volume.

Physical stability study

Backscattering measurements (Turbiscan Lab Expert) were carried out with aging time in order to analyse and quantify the destabilization mechanisms for the emulsions developed. These measurements were performed for at least 25 days at 25°C. Some researchers have quantified the physical stability of emulsions using the Turbiscan Stability Index (TSI) [20,21].

$$TSI = \sum_j \left| scan_{ref}(h_j) - scan_i(h_j) \right| \quad \text{Eq. (3)}$$

where $scan_{ref}$ and $scan_i$ are the initial transmission value and the transmission value at a specific time, respectively and h_j is a specific height in the measuring cell.

Rheological tests

All rheological measurements were performed using a controlled-stress rheometer AR2000 (TA Instruments) equipped by a serrated plate-plate geometry (60 mm of diameter). Small Amplitude Oscillatory Shear tests (SAOS) were conducted from 20 to 0.05 rad/s at a stress in the Linear Visceolastic Range (LVR). The LVR was obtained by means of stress sweeps at 0.1, 1 and 3 Hz. On the other hand, flow curves were carried out by a stress-based multistep protocol (3 min/point) at 20°C. The possible loss of water was avoided using a solvent trap.

Cryo-Scanning Electron Microscopy

Cryo Scanning Electron microscope Zeiss EVO was used in order to observe the microstructure of some selected emulsions with and without diutan gum. Samples were prepared following the protocol reported by Santos et al. [22] and observed at 10 kV.

3. Results and discussion

Comparison between microfluidization and sonication technique for development of lemongrass-in-water emulsions

Figure 1 shows the influence of homogenization pressure and number of cycles on Sauter diameter and span values for lemongrass emulsions processed in Microfluidizer. First at all, it is important to note that the Sauter diameter and the span parameter for the pre-emulsion was 950 ± 50 nm and 0.97, respectively (data not shown). Taking this into account, the reduction of Sauter diameter and span values is very noticeable using microfluidization. The application of 2500 and 5000 psi of homogenization pressure (lower homogenization pressures) in Microfluidizer provoked a decrease of Sauter diameter and span parameter reaching values of 185 nm and 0.7, respectively. However, an increase of both parameter was observed above 5000 psi. This fact is related to the over-processing phenomenon that provokes recoalescence, which is well-known in microfluidizer devices [6,23]. In addition, the increase of number of cycles from one to two cycles at lower pressures did not produce any change in span parameter or Sauter diameter. However, an increment of Sauter diameter with the second cycle was observed at higher pressures. This also points out a recoalescence phenomenon aforementioned. Hence, the application of low homogenization pressures showed the best results concerning Sauter diameter and span parameter, obtaining emulsions with a mean diameter of nanometric size (<200 nm).

Figure 2A illustrates the influence of ultrasonic power used on the Sauter diameter and span parameter for lemongrass-in-water emulsions developed using a sonicator for 3 minutes. The increase of ultrasonic power provoked a decrease in Sauter diameter and span parameter. This fact is due to that higher amplitudes produced more powerful shock waves, which results in smaller Sauter diameters [24].However, a tendency to reach constant values of both parameters at higher amplitudes was detected (Sauter diameter=195 nm; span parameter= 0.8). This tendency has been previously reported by other authors for coconut-in-water emulsions [25]. These results are slight higher than those obtained by microfluidization technique. This same trend was observed for the influence of sonication time on Sauter and span parameter for emulsions developed at 75 W (figure 2B). In conclusion, once the necessary energy to obtain the smallest mean diameter is reached, an increase of energy does not provoke any change. Thus, emulsions prepared using sonicator did not show re-coalescence, conversely to microfluidizer. This fact was previously pointed out by Jafari et al. [8].

Figure 3 shows the Sauter diameter as a function of energy density for all microfluidized and sonicated emulsions. The results obtained demonstrated that the recoalescence phenomenon detected in microfluidized emulsions is not directly related to the energy density. This is supported by the fact that the sonicated emulsion processed at the highest energy density tested did not show over-proccessing. The lack of over-processing in sonicator is probably due to the higher residence times during emulsification. On the other hand, an increase in energy density in microfluidizer involves a decrease in mean residence time of the emulsions in the interaction chamber (in the range of milliseconds) [8]. This could lead to a recoalescence phenomenon because of the possible lack of time in order to get the optimal adsorption of the emulsifier in the interface. Thus, residence time could be the crucial parameter for over-processing. It is also interesting to mark that emulsions produced by sonicator at different amplitudes and times (72 W, 1 min and 32W, 3 min) with similar energy densities (23 and 30 MJ/m^3, respectively) show significant differences in Sauter diameter. This seems to prove that higher amplitudes promote the creation of smaller droplets at similar energy densities. In other words, higher amplitudes with smaller residence times are more efficient that lower amplitudes with higher residence times.

Figure 4 shows the Turbiscan Stability Index (TSI) for emulsions developed using A) microfluidizer at different pressure ,B) sonicator at different ultrasonic power and C) sonicator at different sonication time. TSI was calculated in the low zone of the measuring cell, which is intimately related to a destabilization process by creaming. Interestingly, all emulsions studied underwent the same destabilization process (creaming). In figure 4A, all emulsions studied showed a linear increase in TSI values with aging time. The emulsion that exhibited the lowest slope was processed at the lowest energy density as expected taking into account that its lowest Sauter diameter and span parameter.

Figure 4B shows the influence of ultrasonic power applied in sonicator for 3 minutes on the TSI values with aging time. Firstly, these emulsions processed at higher ultrasonic power exhibited better stabilities against creaming. However, emulsions processed by microfluidizer showed better stability as demonstrated their lower TSI values. Figure 4C presents the influence of sonication time on the TSI values with aging time. TSI values are lower at higher sonication times, showing an enhanced stability in this way. However, this result does not improve the best result obtained for the emulsion processed in Microfluidizer at the lowest energy density. For this reason, this emulsion was selected for a further study that analyse the addition of diutan gum.

Influence of diutan gum concentration on the selected lemongrass-in-water nanoemulsion

Figure 5 illustrates the frequency sweep for microfluidized nanoemulsion previously selected as a function of diutan gum concentration. Firstly, it is important to note that the nanoemulsion without diutan gum did not present measurable viscoelastic properties. A predominance of the elastic modulus, G’, over the viscous modulus, G’’, at higher frequencies was presented for emulsions containing diutan gum. Nevertheless, a crossover point was observed at lower frequencies for 0.2wt% diutan gum emulsion. This point trend to shift progressively to lower frequencies with increasing gum concentration. These systems showed weak gel-like properties in all studied frequency range. This gel-like behaviour could reduce the droplets movement and therefore, the aforementioned creaming process. In addition, an increase in diutan gum concentration provoked an increase in viscoelastic functions. This fact suggests the formation of a network composed by diutan gum, similarly to other gums behaviour [26]. Interestingly, the values and the tendency of the viscoelastic functions for diutan gum emulsions are quite similar that those for diutan gum solutions with 0.5 wt% NaCl [27].

Figure 6 exhibits the flow properties for the selected microfluidized emulsions as a function of diutan gum concentration. First at all, it is important to mention that the emulsion formulated without diutan gum showed Newtonian flow behaviour. This fact has previously reported by other authors for emulsions containing different essential oils [1] . The addition of diutan gum to the selected emulsion provoked the occurrence of shear-thinning behaviour. This flow behaviour is fitted fairly well to Cross model (R^2>0.99; Equation 4).

$$\eta = \frac{\eta_0 - \eta_\infty}{1+(k\cdot\dot{\gamma})^{1-n}} \text{ Eq.(4)}$$

where k in the inverse of critical shear rate for the onset of shear-thinning response, η_0 is the zero-shear viscosity and n is the so-called flow index.

Fitting parameters for this model are shown in table 1. An increase of zero shear viscosity with diutan gum concentration was observed, which is consistent with the mechanical spectra for these emulsions. In addition, there is a tendency of flow index reduction with diutan gum concentration. This fact is also related to a higher structuration grade. Furthermore, emulsions containing diutan gum present a lack of shear rates information of at least two decades, which reveals a relatively subtle very shear-thinning behaviour. This is normally related to the occurrence of a yield point. Although the presence of a yield point is not sufficiently clear in this case, other authors have previously observed it for liquid paraffin nanoemulsions containing diutan gum [19]. These authors pointed out that the occurrence of the yield point of diutan gum emulsions is related to the network structure of the continuous phase.

Table 2. Flow curves fitting parameters for the Cross model for studied emulsions as a function of diutan gum concentration.

wt% Diutan gum	η_o (Pa · s)	η_∞ (Pa · s)	k (s)	n
0.2	28.1	0	28	0.15
0.3	118	0	66	0.12
0.4	253	0.002	58	0.10

Figure 7A shows the increment of Backscattering (BS) at 25 days of aging time for both the selected microfluidized emulsion and the emulsion that contains the highest concentration of diutan gum studied. The microfluidized emulsion illustrates a great drop of BS in the low zone and a marked increase in the top zone of the measuring cell, which are related to the processes of creaming and oiling-off, respectively. The addition of diutan gum reduced considerably the creaming process. However, a bit decrease in BS in the top zone was observed. This could be attributed to a oiling off.

The global Turbiscan Stability Index parameter is shown in figure 7B. This parameter allows all those destabilization processes involved to be globally quantified and compared. As previously explained, emulsion without diutan gum presented a linear increase in TSI with aging time. Conversely, TSI values of emulsions with diutan gum showed a tendency to reach constant values above 20 days of aging time. Thus, emulsions formulated with diutan gum presented an enhanced physical stability. 0.2 wt% and 0.3 wt% diutan gum emulsions presented similar behaviours concerning stability and emulsion with the highest diutan gum concentration showed the best result of stability.

Figure 8 illustrates the droplet size distributions for lemongrass-in-water emulsions as a function of diutan gum concentration. The addition of diutan gum (0.2 and 0.3 wt%) provoked the occurrence of a second peak in the DSD (above 1 µm) related to the widely known partial recoalescence phenomenon during the processing of the gum incorporation. It is important to note that the emulsion containing 0.4 wt% of diutan gum showed a movement of the mean peak in the DSD to higher values of diameters centred at 0.9 µm. This fact could be explained by the displacement of the surfactant by the diutan gum from the interface to the bulk of the continuous phase. This movement would provoke a lack of interface protection, which leads to the total recoalescence phenomenon and therefore, an increase of droplet sizes.

The microstructures observed by Cryo-SEM technique for A) the selected microfluidized emulsion without diutan gum, B,C) 0.2 wt% diutan gum emulsion and D) 0.4 wt% diutan gum emulsion are shown in figure 9. Figure 9A shows the occurrence of isolated droplets of lemongrass essential oil in the continuous phase. The lack of interaction between droplets and the fact of the continuous phase is water and surfactant support the Newtonian flow behaviour of the emulsion. Figures 9B and C present the microstructure for emulsions containing 0.2 wt% of diutan gum at different magnifications. A 3D network formed by diutan gum with two different population of droplets embedded is observed. The higher size of droplets (figure 9C) corresponds to the second peak detected by laser diffraction. 0.4 wt% diutan gum emulsion shows a very similar microstructure than 0.2 wt% diutan gum emulsion. However, the network presented is more compacted and the droplets are bigger, which supports laser diffraction results.

Conclusions

The main aim of this work was to make a comparison of two different techniques such as microfluidization and sonication for producing nanoemulsions formulated with lemongrass essential oil and applyclean 6552. Results obtained by using microfluidization revealed a recoalescence phenomenon at higher pressures tested. However, this destabilization mechanism was not detected in emulsions prepared by sonication despite the high energies input reached. Further analysis of the results demonstrated that at similar values of energy input supplied by both preparation methods provoked recoalescence in microfluidized emulsions, conversely to sonicated emulsions. This fact has been explained in terms of the higher residence times achieved in sonication. All emulsions, regardless of the homogenization method used, underwent creaming with aging time. Nevertheless, the emulsion processed at the lowest homogenization pressure in microfluidizer showed the lowest creaming rate. As strategy to enhance the physical stability of this emulsion, diutan gum was incorporated. The addition of diutan gum provoked the occurrence of viscoelastic properties, showing a weak gel-like behaviour in all the cases. A trend to cross-over point at lower frequencies was detected for 0.3 and 0.4 wt% diutan gum and this point was reached for 0.2 wt% diutan gum at 0.65 rad/s. This indicates a higher grade of structuration in more gum concentrated emulsions. The incorporation of diutan gum to the formulation promoted a substantial improvement of physical stability against creaming. Nevertheless, the emulsion formulated with diutan gum above 0.3 wt% showed coalescence just after preparation with the subsequent increase of droplet size (above 1 µm). Therefore, it is important to reach a balanced compromise on both droplet size and physical stability. These differences of droplet sizes were also evident in the microstructure observed by Cryo-SEM technique, which as well as revealing the existence of a 3D network developed by diutan gum.

Acknowledgements

The financial support received (Project CTQ2015-70700-P) from the Spanish Ministerio de Economia y Competitividad and the European Commission (FEDER Programme) is kindly acknowledged.

References

(1) Santos, J.; Jimenez, M.; Calero, N.; Alfaro, M. C.; Muñoz, J. Influence of a shear post-treatment on rheological properties, microstructure and physical stability of emulgels formed by rosemary essential oil and a fumed silica. *Journal of Food Engineering* **2019**, *241*, 136–148.

(2) Pérez-Córdoba, L. J.; Norton, I. T.; Batchelor, H. K.; Gkatzionis, K.; Spyropoulos, F.;

Sobral, P. J. A. Physico-chemical, antimicrobial and antioxidant properties of gelatin-chitosan based films loaded with nanoemulsions encapsulating active compounds. *Food Hydrocolloids* **2018**, *79*, 544–559.

(3) Trujillo-Cayado, L. A.; Alfaro, M. C.; Santos, J.; Calero, N.; Muñoz, J. Influence of primary homogenization step on microfluidized emulsions formulated with thyme oil and Appyclean 6548. *Journal of Industrial and Engineering Chemistry* **2018**.

(4) Perrier-Cornet, J. M.; Marie, P.; Gervais, P. Comparison of emulsification efficiency of protein-stabilized oil-in-water emulsions using jet, high pressure and colloid mill homogenization. *Journal of Food Engineering* **2005**, *66* (2), 211–217.

(5) Trujillo-Cayado, L. A.; Santos, J.; Alfaro, M. C.; Calero, N.; Muñoz, J. A further step in the development of oil-in-water emulsions formulated with a mixture of green solvents. *Industrial & Engineering Chemistry Research* **2016**, *55* (27), 7259–7266.

(6) Jafari, S. M.; Assadpoor, E.; He, Y.; Bhandari, B. Re-coalescence of emulsion droplets during high-energy emulsification. *Food Hydrocolloids* **2008**, *22* (7), 1191–1202.

(7) Peshkovsky, A. S.; Peshkovsky, S. L.; Bystryak, S. Scalable high-power ultrasonic technology for the production of translucent nanoemulsions. *Chemical Engineering and Processing: Process Intensification* **2013**, *69*, 77–82.

(8) Jafari, S. M.; He, Y.; Bhandari, B. Production of sub-micron emulsions by ultrasound and microfluidization techniques. *Journal of Food Engineering* **2007**, *82* (4), 478–488.

(9) Nejatian, M.; Abbasi, S.; Kadkhodaee, R. Ultrasonic-assisted fabrication of concentrated triglyceride nanoemulsions and nanogels. *Langmuir* **2018**, *34* (38), 11433–11441.

(10) Lago, A. M. T.; Neves, I. C. O.; Oliveira, N. L.; Botrel, D. A.; Minim, L. A.; de Resende, J. V. Ultrasound-assisted oil-in-water nanoemulsion produced from Pereskia aculeata Miller mucilage. *Ultrasonics sonochemistry* **2019**, *50*, 339–353.

(11) Badawy, M. E. I.; Saad, A.-F. S. A.; Tayeb, E.-S. H. M.; Mohammed, S. A.; Abd-Elnabi, A. D. Optimization and characterization of the formation of oil-in-water diazinon nanoemulsions: Modeling and influence of the oil phase, surfactant and sonication. *Journal of Environmental Science and Health, Part B* **2017**, *52* (12), 896–911.

(12) Basak, S.; Guha, P. A review on antifungal activity and mode of action of essential oils and their delivery as nano-sized oil droplets in food system. *Journal of food science and technology* **2018**, 1–10.

(13) Granata, G.; Stracquadanio, S.; Leonardi, M.; Napoli, E.; Consoli, G. M. L.; Cafiso, V.; Stefani, S.; Geraci, C. Essential oils encapsulated in polymer-based nanocapsules as potential candidates for application in food preservation. *Food chemistry* **2018**, *269*, 286–292.

(14) Liakos, I.; Rizzello, L.; Scurr, D. J.; Pompa, P. P.; Bayer, I. S.; Athanassiou, A. All-natural composite wound dressing films of essential oils encapsulated in sodium alginate with antimicrobial properties. *International journal of pharmaceutics* **2014**, *463* (2), 137–145.

(15) Rojas-Graü, M. A.; Raybaudi-Massilia, R. M.; Soliva-Fortuny, R. C.; Avena-Bustillos, R. J.; McHugh, T. H.; Martín-Belloso, O. Apple puree-alginate edible coating as carrier of antimicrobial agents to prolong shelf-life of fresh-cut apples. *Postharvest biology and Technology* **2007**, *45* (2), 254–264.

(16) Natrajan, D.; Srinivasan, S.; Sundar, K.; Ravindran, A. Formulation of essential oil-loaded chitosan–alginate nanocapsules. *journal of food and drug analysis* **2015**, *23* (3), 560–568.

(17) Salvia-Trujillo, L.; Rojas-Graü, M. A.; Soliva-Fortuny, R.; Martín-Belloso, O. Effect of processing parameters on physicochemical characteristics of microfluidized lemongrass essential oil-alginate nanoemulsions. *Food Hydrocolloids* **2013**, *30* (1), 401–407.

(18) Martin-Piñero, M. J.; Ramirez, P.; Muñoz, J.; Alfaro, M. C. Development of rosemary essential oil nanoemulsions using a wheat biomass-derived surfactant. *Colloids and Surfaces B: Biointerfaces* **2019**, *173* (April 2018), 486–492.

(19) Xu, L.; Qiu, Z.; Gong, H.; Liu, C.; Li, Y.; Dong, M. Effect of diutan microbial polysaccharide on the stability and rheological properties of O/W nanoemulsions formed with a blend of Span20-Tween20. *Journal of Dispersion Science and Technology* **2018**, *39* (11), 1644–1654.

(20) Raikos, V. Encapsulation of vitamin E in edible orange oil-in-water emulsion beverages: Influence of heating temperature on physicochemical stability during chilled storage. *Food Hydrocolloids* **2017**.

(21) Santos, J.; Calero, N.; Trujillo-Cayado, L. A.; Garcia, M. C.; Muñoz, J. Assessing differences between Ostwald ripening and coalescence by rheology , laser diffraction and multiple light scattering. *Colloids and Surfaces B : Biointerfaces* **2017**, *159*, 405–411.

(22) Santos, J.; Calero, N.; Trujillo-Cayado, L.; Alfaro, M. C.; Muñoz, J. The Role of Processing Temperature in Flocculated Emulsions. *Industrial & Engineering Chemistry Research* **2017**.

(23) Jafari, S. M.; He, Y.; Bhandari, B. Optimization of nano-emulsions production by microfluidization. *European Food Research and Technology* **2007**, *225* (5-6), 733–741.

(24) Maherani, B.; Khlifi, M. A.; Salmieri, S.; Lacroix, M. Design of biosystems to provide healthy and safe food. Part A: effect of emulsifier and preparation technique on physicochemical, antioxidant and antimicrobial properties. *European Food Research and Technology* **2018**, *244* (11), 1963–1975.

(25) Ramisetty, K. A.; Pandit, A. B.; Gogate, P. R. Ultrasound assisted preparation of emulsion of coconut oil in water: understanding the effect of operating parameters and comparison of reactor designs. *Chemical Engineering and Processing: Process Intensification* **2015**, *88*, 70–77.

(26) Xu, L.; Xu, G.; Liu, T.; Chen, Y.; Gong, H. The comparison of rheological properties of aqueous welan gum and xanthan gum solutions. *Carbohydrate Polymers* **2013**, *92* (1), 516–522.

(27) Carmen García, M.; Trujillo, L. A.; Carmona, J. A.; Muñoz, J.; Carmen Alfaro, M. Flow, dynamic viscoelastic and creep properties of a biological polymer produced by Sphingomonas sp. as affected by concentration. *International Journal of Biological Macromolecules* **2018**, No. xxxx.

Figures with captions

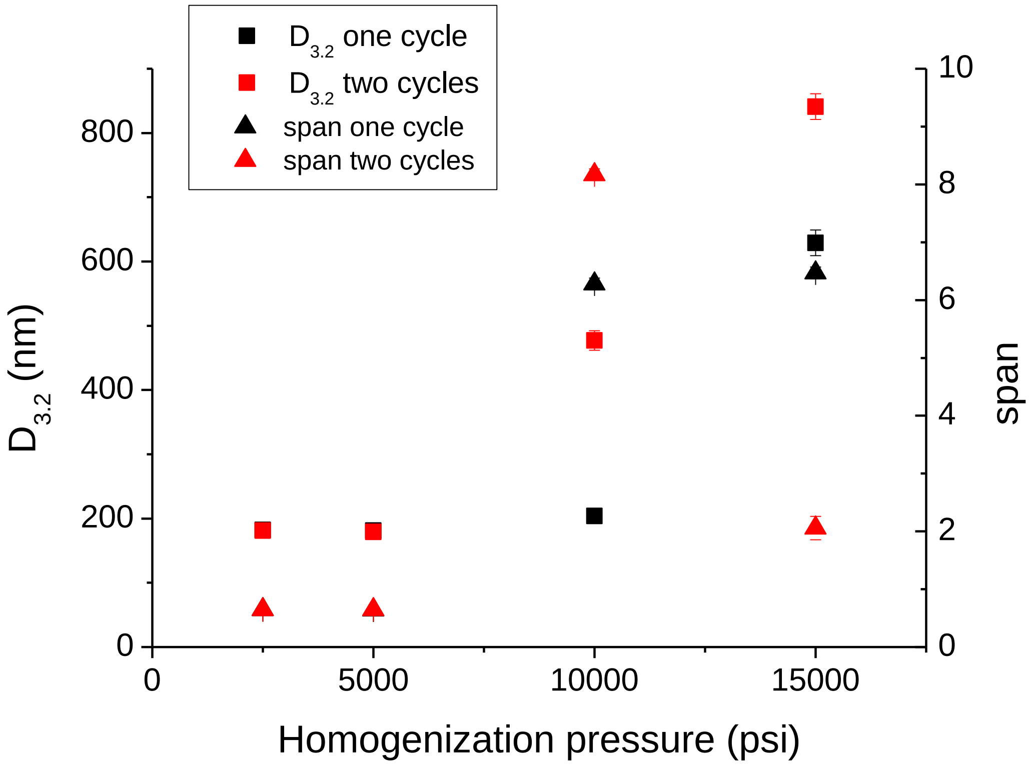

Figure 1. Influence of homogenization pressure and number of cycles on Sauter diameter and span for lemongrass emulsions.

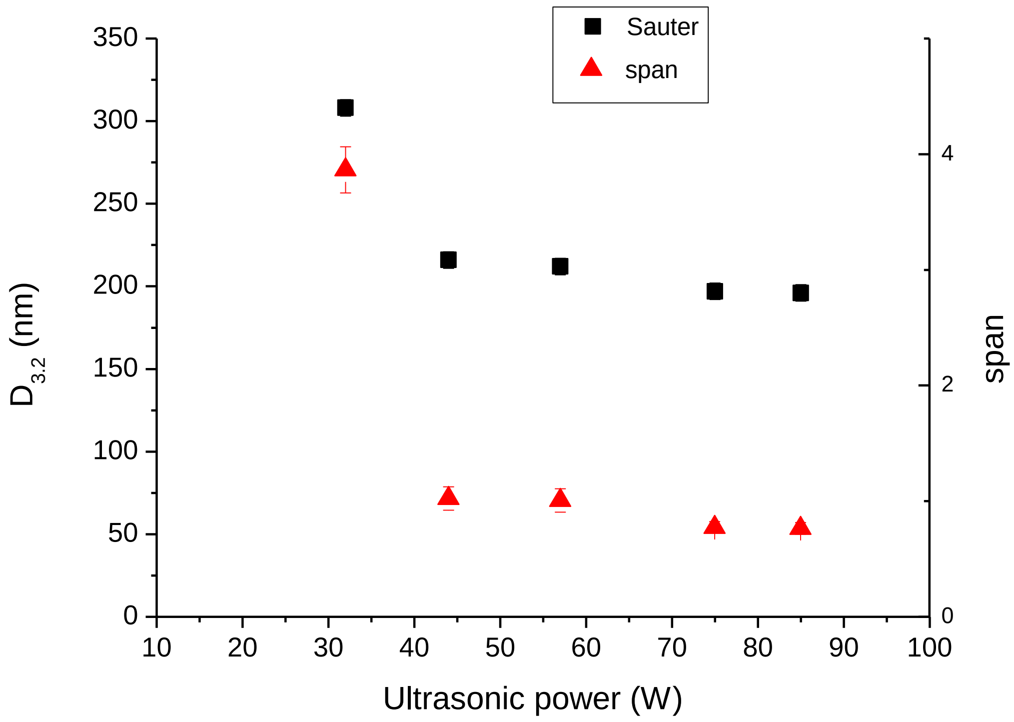

Figure 2A. Influence of ultrasonic power on Sauter diameter and span values for lemongrass emulsions processed in sonicator for 3 minutes.

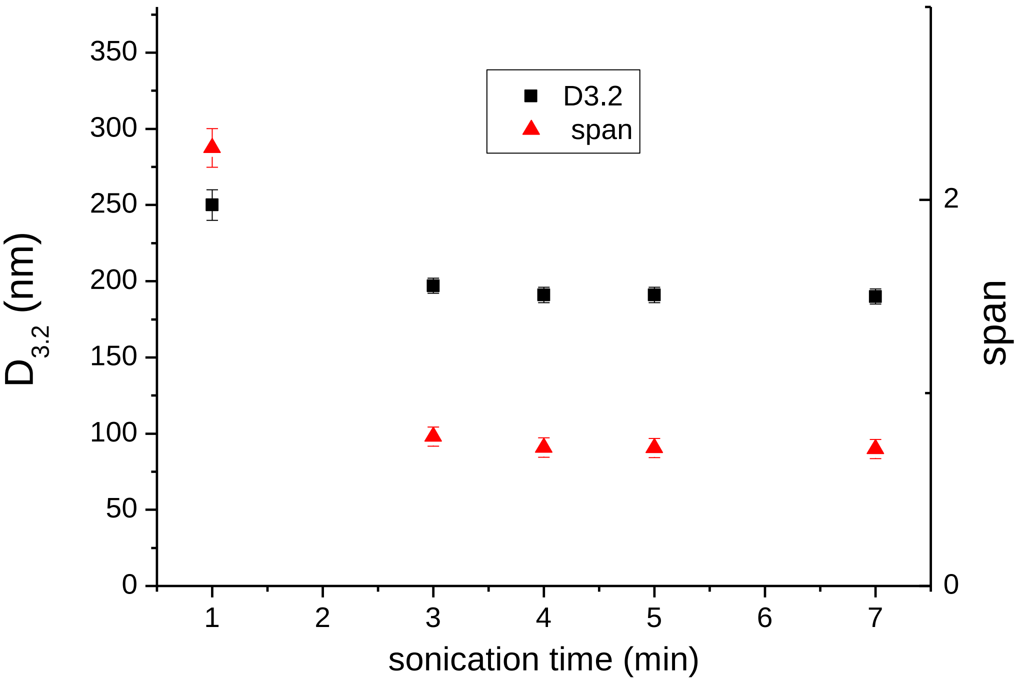

Figure 2B. Influence of sonication time on Sauter diameter and span values for lemongrass emulsions processed in sonicator at 75 W.

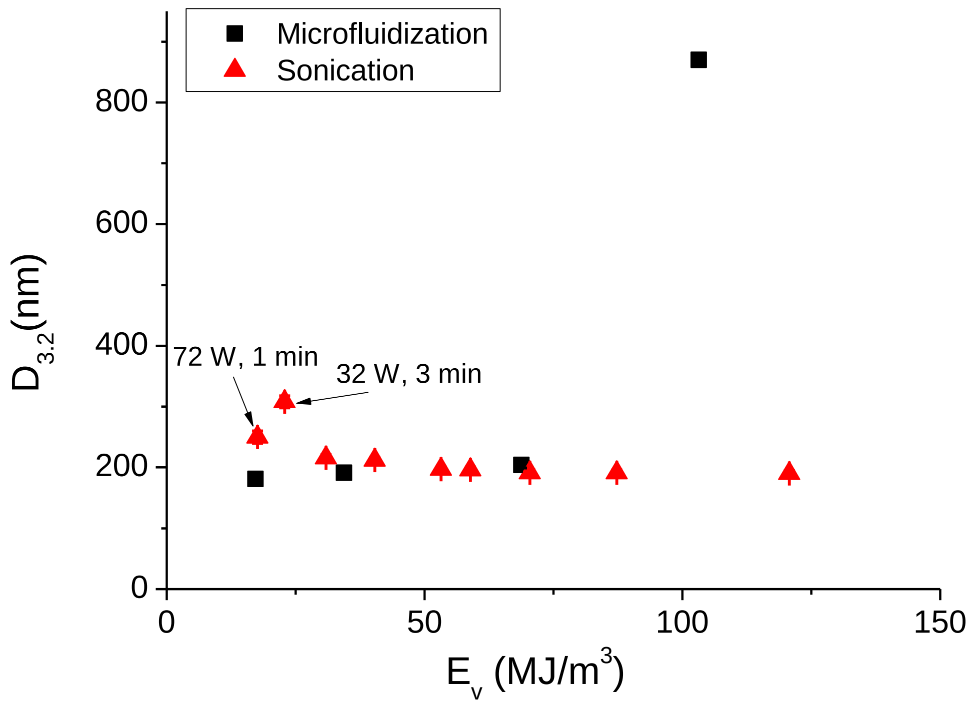

Figure 3. Sauter diameter obtained as a function of energy input for lemongrass-in-water emulsions.

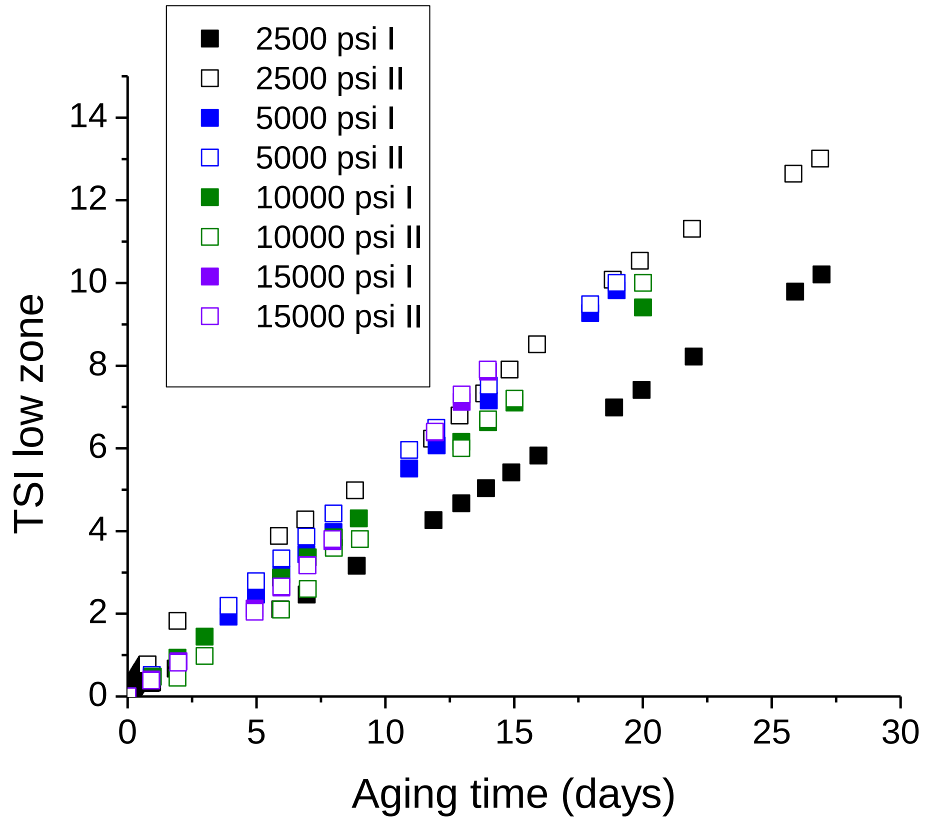

Figure 4A. TSI values in the low zone with aging time as a function of homogenization pressure and number of cycles applied in Microfluidizer.

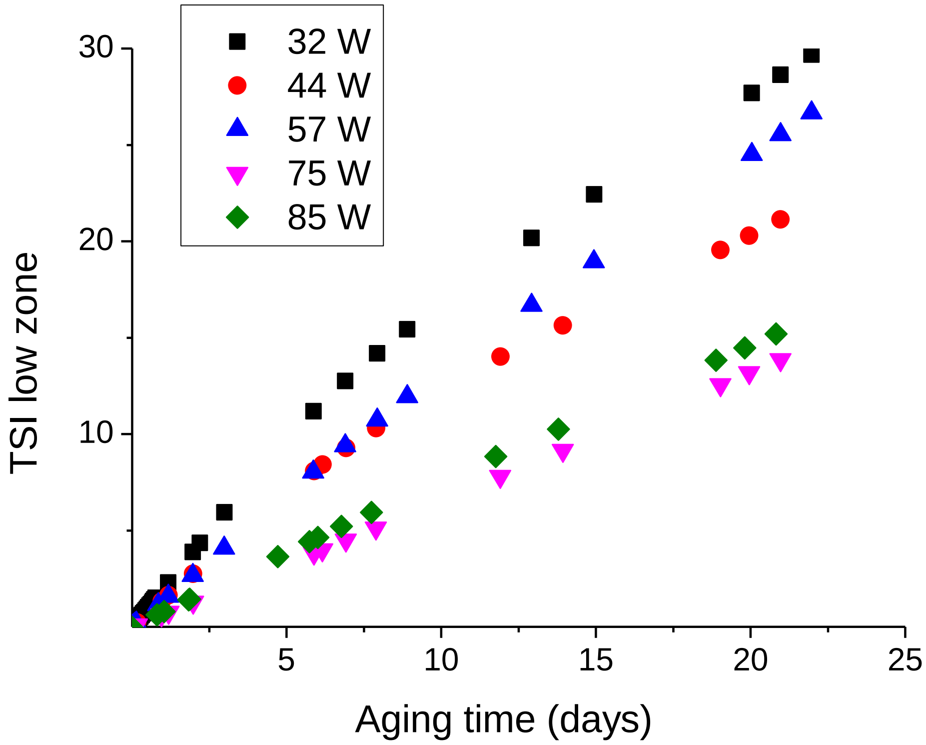

Figure 4B. TSI values in the low zone with aging time as a function of ultrasonic power applied in sonicator for 3 minutes.

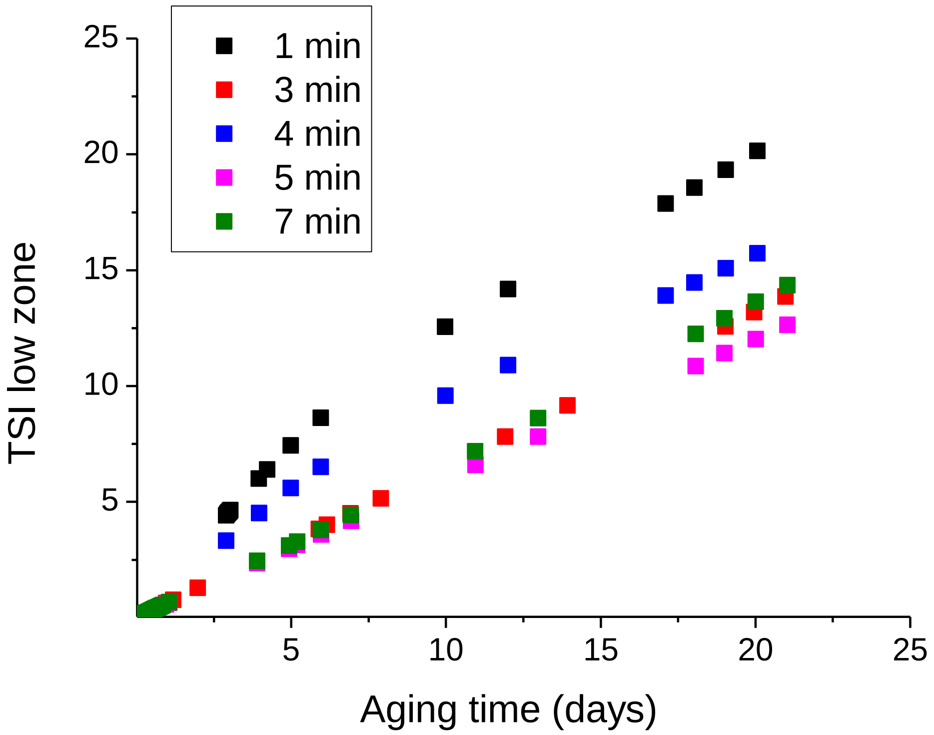

Figure 4C. TSI values in the low zone with aging time as a function of ultrasonic power applied in sonicator for 3 minutes.

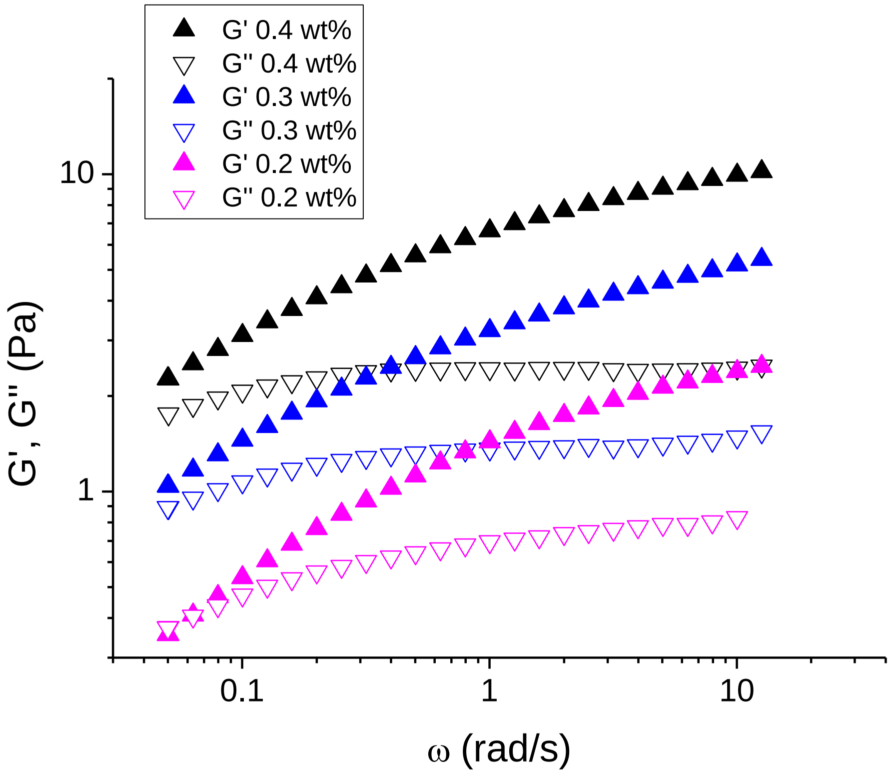

Figure 5. Mechanical spectra for lemongrass-in-water emulsions as a function of diutan gum concentration at 20°C.

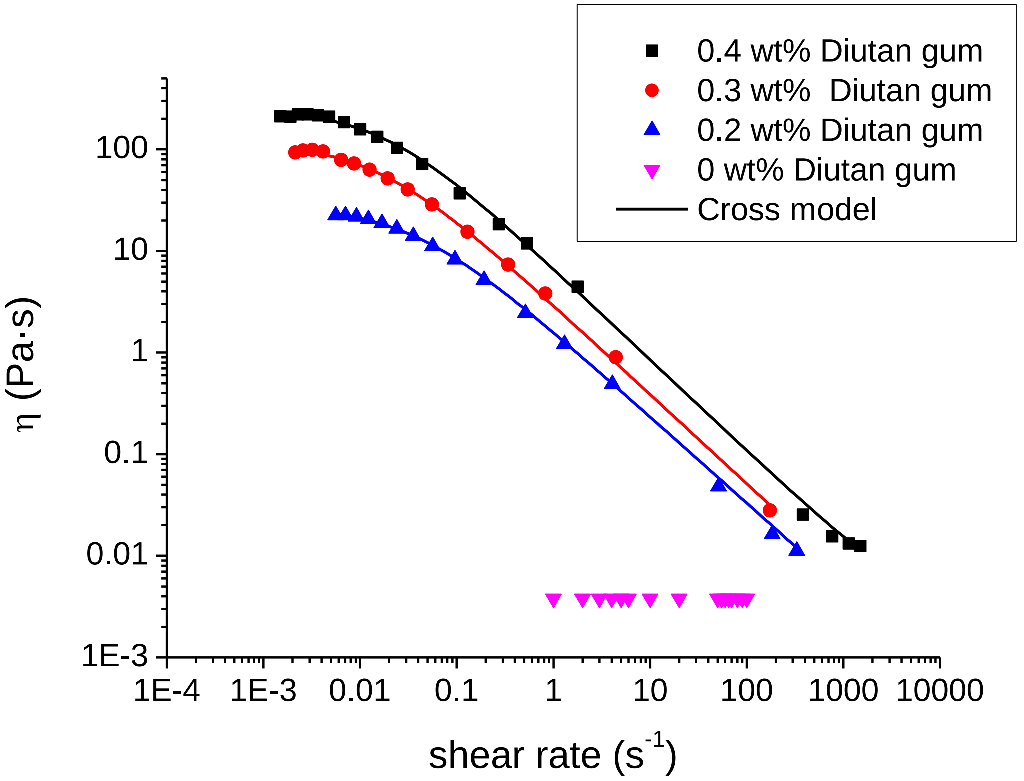

Figure 6. Flow curve for lemongrass-in-water emulsions as a function of diutan gum concentration.

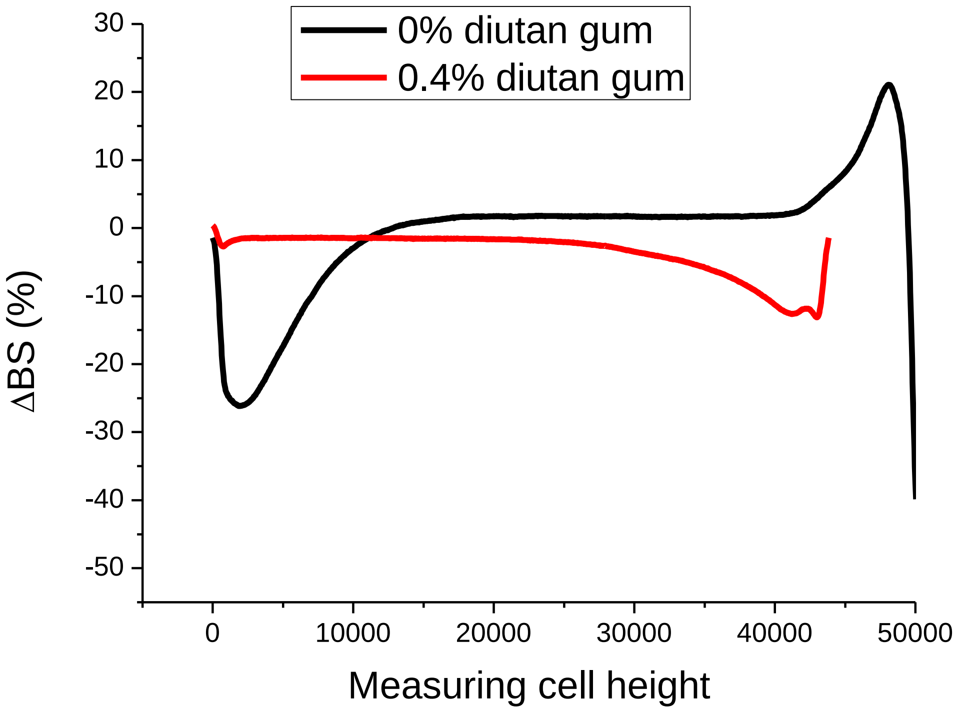

Figure 7A. Backscattering variation as a function of measuring cell height for emulsions without and with 0.4 wt% of diutan gum at 25 days of aging time.

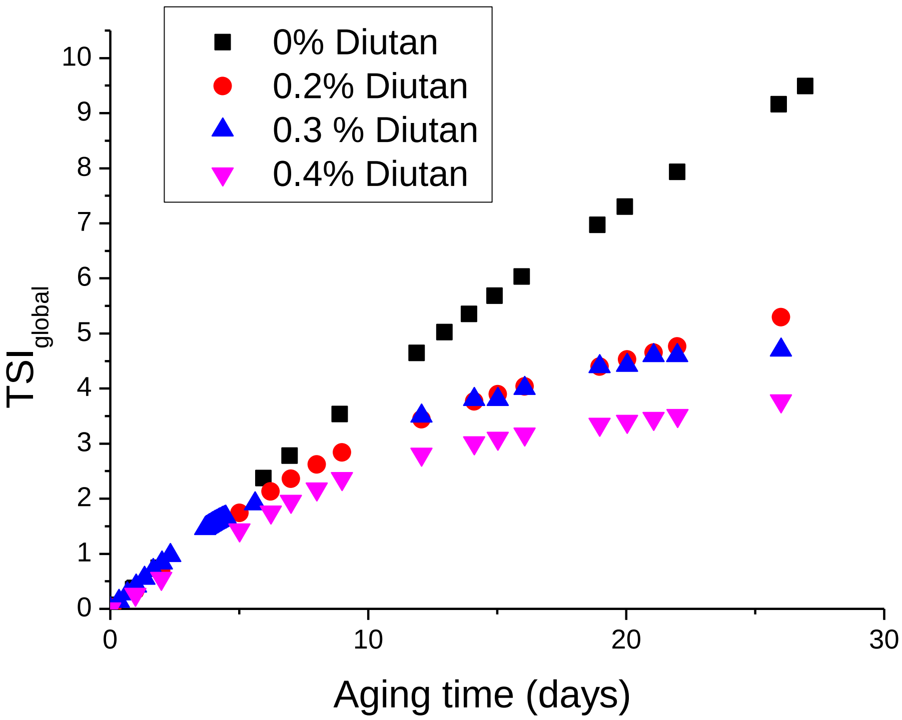

Figure 7B. Global Turbiscan Stability Index (TSI) with aging time as a function of diutan gum concentration for lemongrass-in-water emulsions.

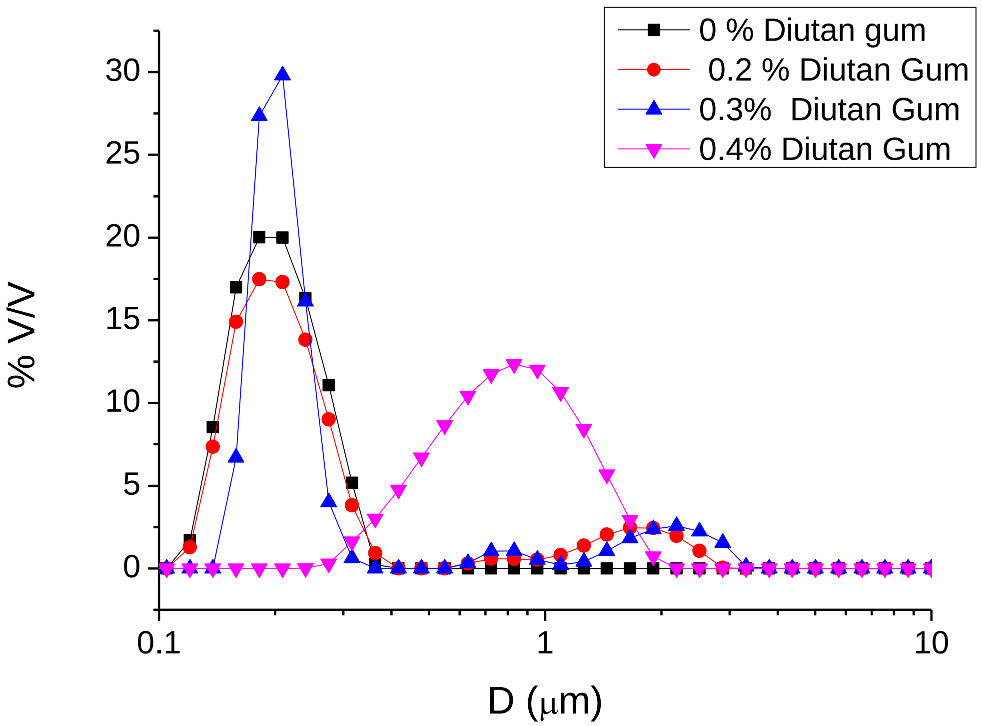

Figure 8. Droplet size distributions for lemongrass-in-water emulsions as a function of diutan gum.

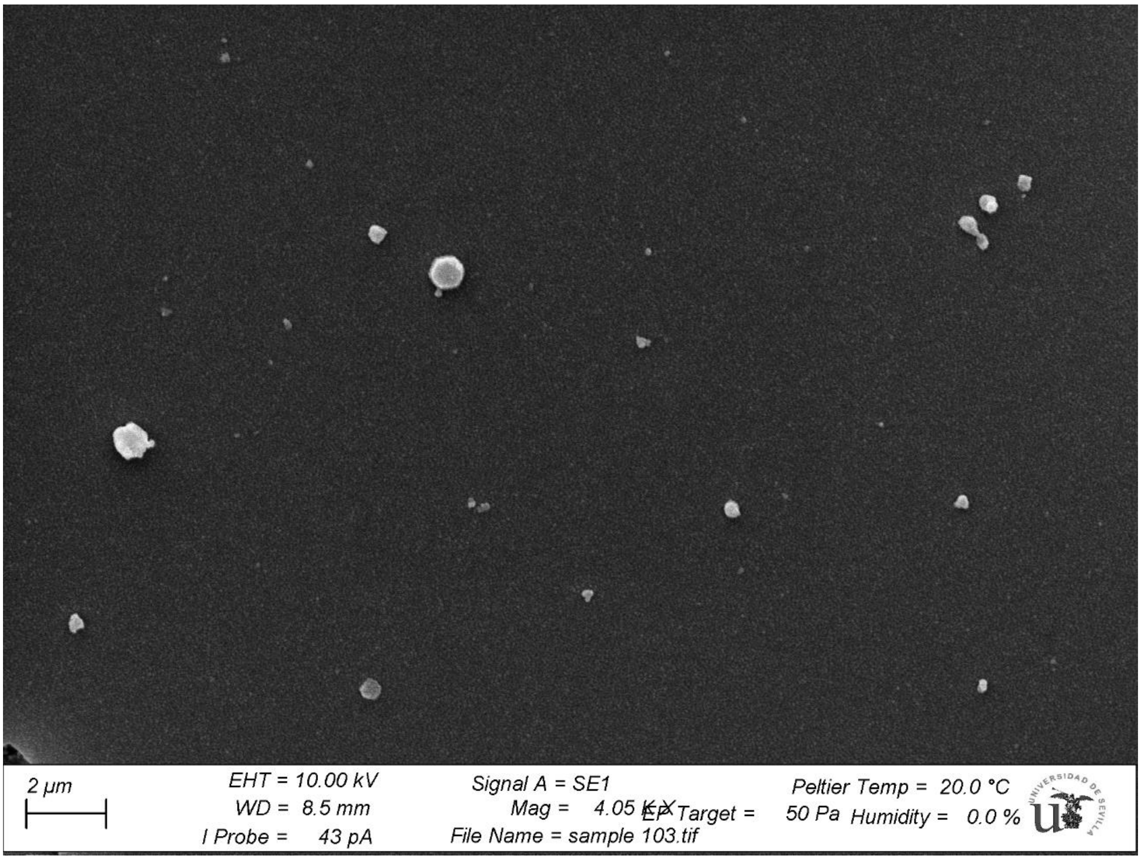

Figure 9A. Microstructure of the selected microfluidized lemongrass-in-water emulsion observed by Cryo-SEM technique.

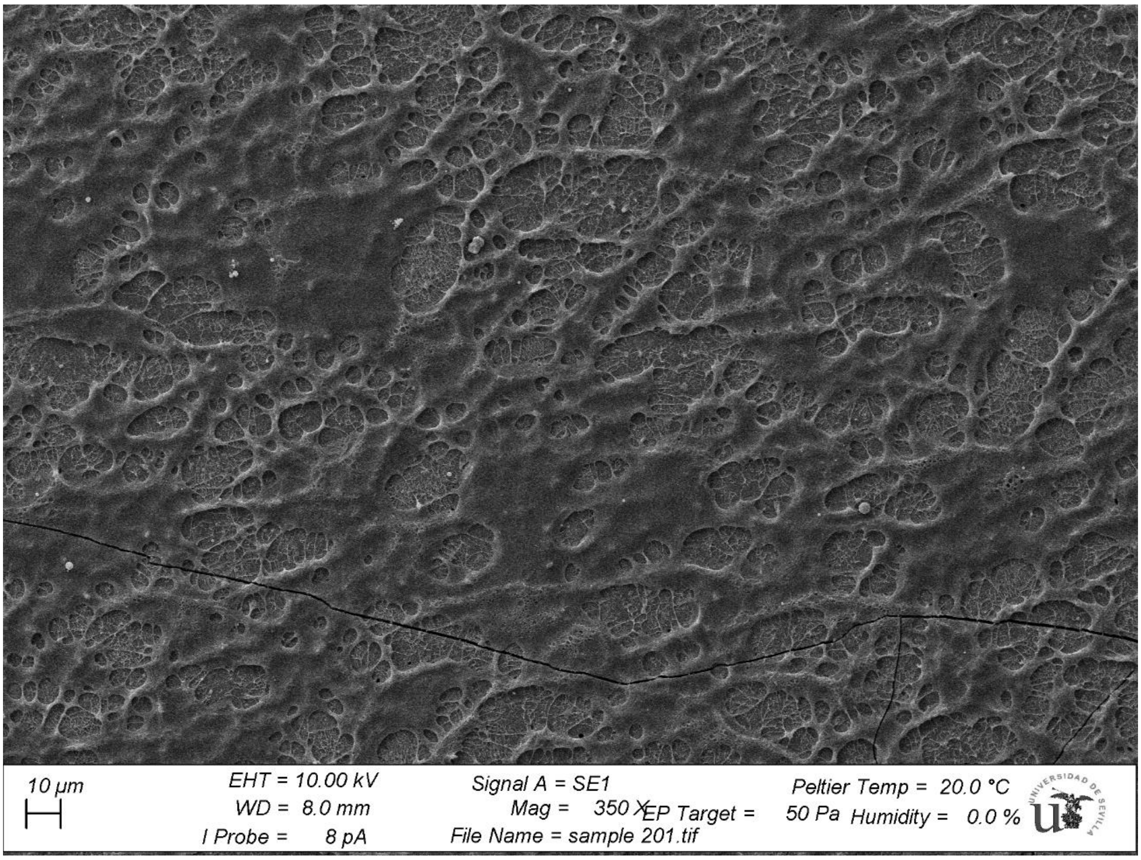

Figure 9B. Microstructure of lemongrass-in-water emulsion containing 0.2wt% diutan gum observed by Cryo-SEM technique at 350X.

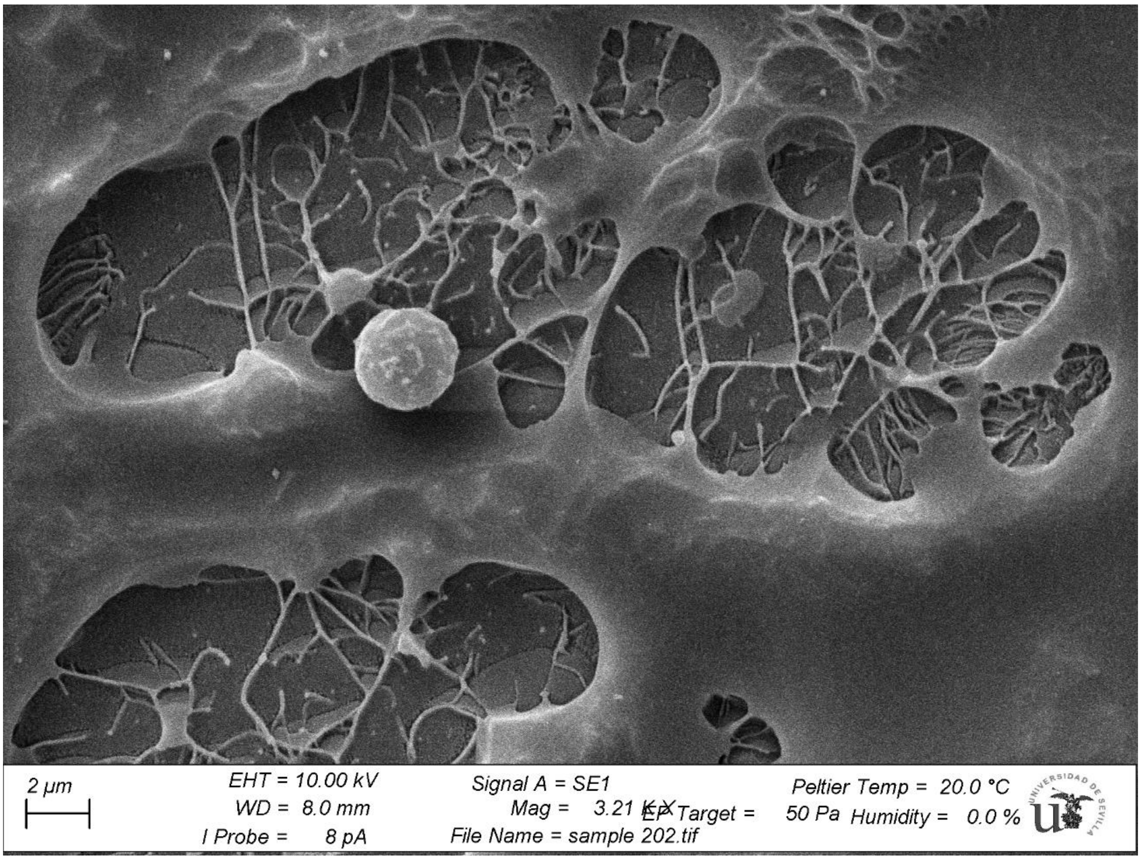

Figure 9C. Microstructure of lemongrass-in-water emulsion containing 0.2 wt% diutan gum observed by Cryo-SEM technique at 3.21 KX.

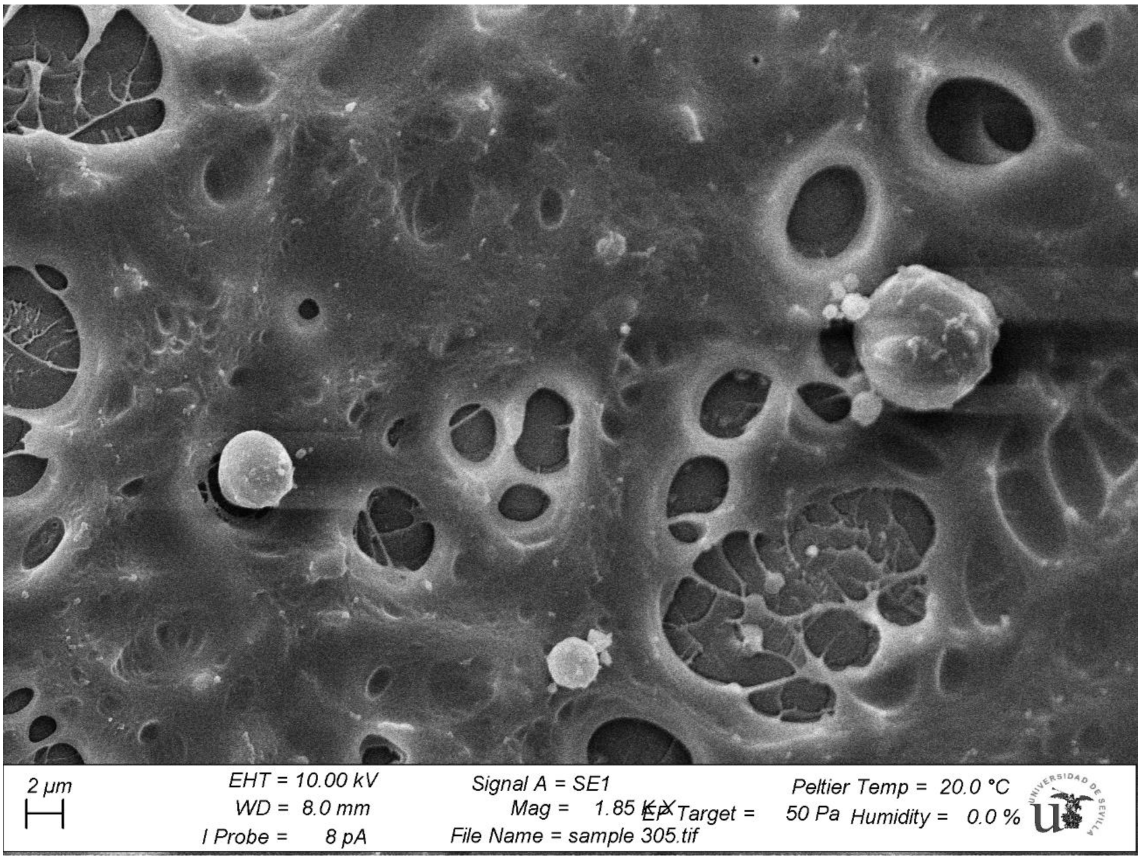

Figure 9D. Microstructure of lemongrass-in-water emulsion containing 0.4 wt% diutan gum observed by Cryo-SEM technique at 1.85KX.